2018 IEEE-RAS 18th International Conference on Humanoid Robots (Humanoids)
Beijing, China, November 6-9, 2018

Natural Oscillation and Optimal Gaits for Humanoid Biped Models

Uzair Ijaz Khan and Zhiyong Chen

Abstract— **Gait design for a biped robot is an intriguing problem. The objective is to replicate an efficient gait according to the jogging dynamics of a human in a biped robot. This paper aims to find an optimal gait for jogging dynamics of a biped robot on a continuous-time nonlinear mathematical model. The nonlinear model is approximated using the describing function method and requires the gait to be sinusoidal. It is revealed that the natural oscillation of an undamped biped robot is also an optimal gait. The optimal frequency reduces to compensate for damping. The characteristic of the optimal gait is further studied in extensive simulations.**

I. Introduction

Control engineers often look for inspiration in nature to solve their complex design problems. Gait design for a robot is a challenging problem for which one can turn to animal locomotion. More often than not, gaits used by animals minimize some sort of cost function or performance criterion such as energy. This makes it intriguing to analyze these gaits. This analysis not only aids us in designing gaits for a robotic locomotor but also gives us an insight into animal locomotion. The specific task in this paper is to find out if the gait naturally defined by a biped robot's dynamic structure is an optimal gait.

Biped walkers are of profound interest these days. A review of such models were presented in, e.g., [1] and [2], to analyze human like walking. The pioneering work on such walkers was initiated by Tad McGeer [3] who investigated the passive gait through mathematical modelling. Following the work, Goswami et al. [4] produced a series of literature based on a class of biped walkers, which were known as compass-gait walkers due the resemblance to a compass, while utilizing event based impact models. More recently, walking and running of energy efficient planar passive bipeds was studied in [5], [6]. Compass-gait biped has emerged as a test bench for control strategies in legged locomotion in the last two decades [7]. Lately, stable walking using model predictive control was proposed in [8], while [9] and [10] proposed effective pattern generation for walking of bipeds.

The use of event-based impact modeling, in the case of biped modeling, leads to a hybrid model, as is the case in [11]. This often means that the gait is divided into two phases: a swing stage and an instantaneous transition stage. The kinematics of such a hybrid model are simple. However, its analysis is quite complicated because of the presence of discontinuous terms in the differential equation. Hence, continuous-time mathematical models were developed to remedy this difficulty. One such a model was presented in [12] which utilizes force-based contact model. Similarly, a new mathematical model was discussed in our preceding work [13] whereby a nonlinear saturation function caters for the discontinuities resulted by the impact. This model ensures that the dynamics are captured in one differential equation, hence eliminating the need for an inconvenient hybrid model. Also in [13], a class of natural oscillation was defined for this continuous-time biped model. The idea of natural oscillation for a biped model can be traced back to the natural oscillation for the mechanical locomotion systems studied in [14], [15] and even back to the traditional natural frequency of a simple pendulum. But it remains to be answered if a biped gait in natural oscillation optimizes some performance criterion or cost function.

It is not always possible to find the globally optimal solution to general optimal control problems. Most of the commonly used methods guarantee local optimality at best, which means the optimal solution depends on the initial conditions of the numerical search, and hence could be far from the global optimum. One of the commonly used methods is to apply the calculus of variations, as done in [16], [17]. Another commonly used method involves expansion of signal over a finite set of basis functions. This method was used for optimal control of a biped walker in [18].

In this paper, we take a different approach that was developed in [19], whereby a nonlinear model was simplified first and then a method was developed to find the optimal gait. However, it focussed primarily on systems continually interacting with the environment which is not the case for a walking or a jogging robot. The fully nonlinear model developed in [13] needs to be tailored using the describing function with hysteresis before an optimal gait is computed. It is revealed that the natural oscillation defined in [13] for an undamped biped robot is also an optimal gait in terms of minimizing control input torque or torque rate. The optimal frequency reduces to compensate for damping. The result is also verified by extensive simulations.

In this paper, for a complex matrix M, its transpose, conjugate transpose and real parts are denoted by $M^\intercal$, M^* and $\Re[M]$ respectively. The set $\mathbb{P}_T$ represents T-periodic sinusoidal vector valued signals with $T \in \mathbb{R}^+$. For a n-dimensional signal $x(t) = \Re[\hat{x}e^{j\omega t}] \in \mathbb{P}_T$ with $T = 2\pi/\omega$, the vector $\hat{x} \in \mathbb{C}^n$ is called its phasor.

II. Biped models

The first biped model studied in this paper consists of two links, with distributed mass representing each leg, connected together by a hip joint, which represents the upper body

The authors are with the School of Electrical Engineering and Computing, The University of Newcastle, Callaghan, NSW 2308, Australia. Uzair.Khan@uon.edu.au, zhiyong.chen@newcastle.edu.au.

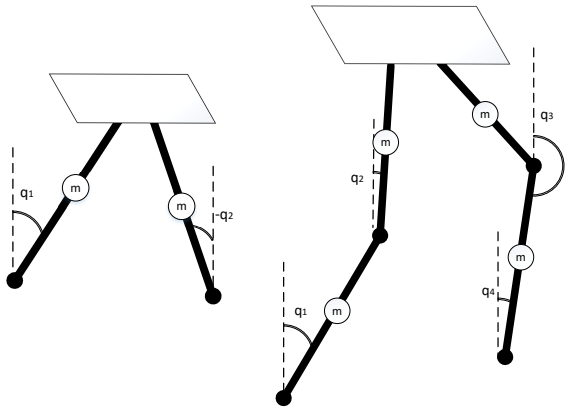

Fig. 1. Schematic diagrams of a compass-like two-link biped robot and a four-link biped robot. [13]

as shown in the left graph of Figure 1. The legs have springs attached beneath them to provide a force at the time of impact. The mathematical model is derived from the standard Euler-Lagrange equation with the details given in the preceding work [13].

Let $q = [q_1, q_2]^\intercal$ be a vector of generalized coordinates in the configuration space as shown in Figure 1. The Lagrangian formula yield the equation of motion

$$J\ddot{q} + C(q,\dot{q})\dot{q} + D(q)\dot{q} + K_o q + G_o(q) = T_c(q,\dot{q}) + u. \quad (1)$$

Here J is a positive definite matrix representing moment of inertia, $C(q,\dot{q})$ and $D(q)$ denote the Coriolis and the damping matrices respectively, K_o represents the joint stiffness, $G_o(q)$ denotes the Gravitational torque, whereas $T_c(q,\dot{q})$ is the torque of the contact force from the ground. For simplicity, the Rayleigh damping ($D = \mu J$) was considered, where μ denotes the damping factor. Approximated at small q and $\dot{q}$, the equation (1) becomes

$$J\ddot{q} + \mu J\dot{q} + (K_o + G_o)q = T_c(q,\dot{q}) + u. \quad (2)$$

In particular, J, K_o, and G_o take appropriate forms on the parameters m, l, k_o, g_o defined in Table I.

The contact torque vector

$$T_c(q,\dot{q}) = \begin{bmatrix} \tau(q_1,\dot{q}_1) \\ \tau(q_2,\dot{q}_2) \end{bmatrix}$$

consists of $\tau(q_i,\dot{q}_i)$ for each leg that is given by

$$\tau(q_i,\dot{q}_i) = l\sin(q_i)\phi(q_i)c(\dot{q}_i).$$

The normal force from the ground through the spring contact is denoted by $\phi(q_i)$ with the following definition

$$\phi(x) = -\gamma\min(h(x) - \epsilon l, 0),\ h(x) = l - l(\cos(x))$$

for two constants ϵ and γ. The springs can only have a maximum compression of ϵl. The maximum compression for each spring is reached when its associated leg angle becomes zero. The functions $h(x)$ and $\phi(x)$ denote the height of the foot and the normal contact force, respectively. The function $c(\dot{q}_i)$ determines which leg is in forward swing motion and which one is meant to be planted, specifically, with the following definition

$$c(x) = \max\{-\text{sign}(x), 0\} = \begin{cases} 0, & x \geq 0 \\ 1, & x < 0 \end{cases}.$$

TABLE I

PARAMETERS OF THE BIPED MODELS

m	Mass of leg (two-link)	5	kg
$m_1 = m_4$	Mass of shank (four-link)	4	kg
$m_2 = m_3$	Mass of thigh (four-link)	20	kg
l	Length of leg	1	m
ϵl	Max. spring compression	4	cm
γ	Spring constant	5000	N/m
μ	Damping coefficient	0.5	s^{-1}
F_n	Knee torque	800	Nm
k_o	Stiffness parameter	50 (two-link)	Nm/rad
		250 (four-link)	Nm/rad
g_o	Gravitational parameter	4.9	N/kg·rad

The second model is a four-link structure, whereby knee joints are added for both legs. The right graph of Figure 1 shows a diagrammatic representation of the model. With $q = [q_1, \cdots, q_4]^\intercal$, the dynamics can be modelled as follows

$$J\ddot{q} + \mu J\dot{q} + (K_o + G_o)q = T_c(q,\dot{q}) + T_k(q) + u \quad (3)$$

where the contact torque vectors are

$$T_c(q,\dot{q}) = \begin{bmatrix} \tau(q_1,q_2,\dot{q}_1) \\ 0 \\ 0 \\ \tau(q_4,q_3,\dot{q}_4) \end{bmatrix}, T_k(q) = \begin{bmatrix} s(q_1 - q_2) \\ 0 \\ 0 \\ s(q_4 - q_3) \end{bmatrix},$$

and $\tau(q_i,q_j,\dot{q}_i) = l\sin(q_i)\phi(q_i,q_j)c(\dot{q}_i)$. The normal force from the ground through the spring contact is denoted by $\phi(q_i,q_j)$ with the following definition

$$\phi(x_1,x_2) = -\gamma\min(h(x_1,x_2) - \epsilon l, 0)$$
$$h(x_1,x_2) = l - 0.5l(\cos(x_1)) - 0.5l(\cos(x_2)).$$

In particular, in (3), J, K_o, and G_o take appropriate forms on the parameters $m_1, m_2, m_3, m_4, l, k_o, g_o$ defined in Table I. One interesting aspect of human gait is provided by the knee caps. The knee caps, represented by $T_k(q)$, differentiate the jogging gait from the dynamics of a double pendulum by preventing the shank leg from exceeding thigh angles. Hence, another force, and subsequently a torque, is needed to realize this knee cap in the model in (3) where, with F_n being the knee torque given in Table I,

$$s(x) = \begin{cases} 0 & x < 0 \\ F_n & x \geq 0 \end{cases}.$$

III. NATURAL OSCILLATION GAIT

It is observed in [13] that sinusoid-like mode usually exists in the response of the biped models. This observation motivates the natural oscillation as follows. The model (2) or (3), with the nonlinear function $T_c(q,\dot{q})$ approximated by $T_c(q,\dot{q}) = Nq$, can be rewritten as

$$J\ddot{q} + \mu J\dot{q} + (K_o + G_o - N)q = 0. \quad (4)$$

A valid approximation $T_c(q,\dot{q}) \approx Nq$ must hold for a sinusoidal oscillation vector $q(t) = z\sin(\omega t)$, that is,

$$T_c(z\sin(\omega t), z\omega\cos(\omega t)) \approx Nz\sin(\omega t).$$

Describing function approximation was used for this purpose in [13]. More specifically, the vector z, i.e., the relative amplitude and phase distribution of $q(t)$, has a typical format

$$z = \alpha\begin{bmatrix}1\\-1\end{bmatrix} \text{ or } z = \alpha\begin{bmatrix}1\\ \beta\\ -\beta\\ -1\end{bmatrix},\ \alpha,\beta\in\mathbb{R}^+,$$

for the two-link or the four-link model, respectively. As a result, the describing function N explicitly depends on α and β, that is, $N(\alpha)$ for a two-link case, and $N(\alpha,\beta)$ for a four-link case. In particular, α denotes the amplitude of the sinusoid for each leg whereas β denotes the ratio of amplitude of thigh and shank links. For the convenience, we only consider the four link case in the subsequent analysis regarding the two link case as a special case with β vanished.

Definition 3.1: Consider the system (4) with an explicit $N(\alpha,\beta)$ for $\alpha,\beta\in\mathbb{R}^+$. The sinusoidal vector signal $q(t) = z_n\sin(\omega_n t)$ is called a *natural oscillation* if

$$\sigma = \omega_n^2,\ z_n = \alpha\begin{bmatrix}1\\ \beta_n\\ -\beta_n\\ -1\end{bmatrix}$$

is real eigenvalue and eigenvector pair of $J^{-1}(K_o + G_o - N(\alpha,\beta_n))$, i.e.,

$$(K_o + G_o - N(\alpha,\beta_n))z_n = \sigma J z_n. \tag{5}$$

In particular, ω_n and z_n are referred to as the *natural frequency* and *mode shape* of the natural oscillation.

It is easy to see that, $q(t) = z\sin(\omega_n t)$ is a sustained solution to the system (4) with $\mu = 0$. The selection of (σ, z), as the eigenvalue/eigenvector pair, is not unique and the one is selected for defining natural oscillation according to its reasonable phase profile. It is noted that the amplitude α plays no role in natural oscillation due to the freedom in selecting α for the eigenvector z.

IV. Optimal Oscillation Gait

The main objective of this paper is to examine whether the natural oscillation is an optimal gait for humanoid biped model and in what sense. For this purpose, let us introduce the following notations.

Consider a class of transfer functions $\Pi(s)$ of the form $\Pi(s) = F(-s)^\intercal\Phi F(s)$ where Φ is a constant Hermitian matrix and $F(s)$ is a linear combination of stable (proper) transfer functions and differentiators. When $F(s)$ is subjected to an input $\mu\in\mathbb{P}_T$, the output is given by $y + \widetilde{y}$ where y is the steady state response that is T-periodic and $\widetilde{y}$ is the transient which eventually dies out. With a slight abuse of notation, we denote the T-periodic signal $y^\intercal\Phi y$ by $\mu^\intercal\overset{o}{\Pi}\mu$. By Lemma 7.1 in Appendix, the average value of $y^\intercal\Phi y$ over a time period is given by $\hat{\mu}^*\Pi(j\omega)\hat{\mu}/2$ when μ is sinusoidal. The reason why we are restricting our attention to sinusoidal gaits is the limitation of the describing function as it requires the input to be sinusoidal.

Consider the biped robot with the equation of motion given in (4) with an explicit $N(\alpha,\beta)$ and an additional u being the control torques applied to the links. Again, the two-link model with $N(\alpha)$ is regarded as a special case with β vanished. We would like to find an *optimal gait*, particularly an optimal frequency represented by $\omega_o = 2\pi/T$ and mode shape represented by β_o, such that the sinusoidal time periodic gait $q(t)$ and the control input $u(t)$ achieving the gait that minimizes a specified quadratic cost function, over a set of feasible constraints. The problem can be rigorously formulated as the following optimization over the set of T-periodic sinusoidal signals for a fixed $\alpha\in\mathbb{R}^+$:

$$\min_{\substack{\omega,\beta\in\mathbb{R}^+\\ u,q\in\mathbb{P}_T,\ T=2\pi/\omega}} \frac{1}{T}\int_0^T \begin{bmatrix}q\\u\end{bmatrix}^\intercal \overset{o}{\Pi}\begin{bmatrix}q\\u\end{bmatrix} dt \text{ subject to}$$
$$\begin{cases} J\ddot{q} + \mu J\dot{q} + (K_o + G_o - N(\alpha,\beta))q = u \\ \hat{q} = \alpha\begin{bmatrix}1\\ \beta\\ -\beta\\ -1\end{bmatrix} \text{ is the phasor of } q(t)\end{cases}. \tag{6}$$

Here q and u belong to a set of sinusoidal signals satisfying the equation of motion, and $\Pi(s)$ is a transfer function corresponding to the objective integral. The objective function turns out to be quadratic in q and u. With a suitable choice of $\Pi(s)$, one can also capture the derivatives of these signals, hence allowing the flexibility to represent many physical quantities. Table II shows the physical quantities represented by the objective functions and the Π matrices.

TABLE II
Objective functions specified by $\Pi(j\omega)$

Quantity	Objective Integral	$\Pi(j\omega)$
Input torque	$\frac{1}{T}\int_0^T \|u\|^2 dt$	$\begin{bmatrix}0 & 0\\ 0 & I\end{bmatrix}$
Input torque rate	$\frac{1}{T}\int_0^T \|\dot{u}\|^2 dt$	$\begin{bmatrix}0 & 0\\ 0 & \omega^2 I\end{bmatrix}$

Next, the optimization problem formulated in (6) is modified to a constrained quadratic optimization problem whose objective function is only a function of input phasor. In the following lemma, It is noted that $n = 4$ is the dimension for the four-link model and it reduces to $n = 2$ for the two-link model with β vanished.

Lemma 4.1: Define

$$X(\omega,\beta) := \frac{1}{2}\begin{bmatrix}P(\omega,\beta)\\ I\end{bmatrix}^* \Pi(j\omega)\begin{bmatrix}P(\omega,\beta)\\ I\end{bmatrix},$$
$$P(\omega,\beta) := (K_o + G_o - N(\alpha,\beta) + j\omega\mu J - \omega^2 J)^{-1}. \tag{7}$$

Then the optimization problem (6) is equivalent to

$$\min_{\substack{\omega,\beta\in\mathbb{R}^+\\ \hat{u}\in\mathbb{C}^n}} \hat{u}^* X(\omega,\beta)\hat{u} \text{ subject to}$$

$$P(\omega,\beta)\hat{u} = \alpha \begin{bmatrix} 1 \\ \beta \\ -\beta \\ -1 \end{bmatrix} \tag{8}$$

where $u, q \in \mathbb{P}_T$ in (6) are given by

$$u(t) = \Re[\hat{u}e^{j\omega t}], \quad q(t) = \Re[P(\omega,\beta)\hat{u}e^{j\omega t}]. \tag{9}$$

Proof: Let $\hat{q}$ and $\hat{u}$ be phasors of periodic signals $q(t)$ and $u(t)$ respectively. The first constraint of (6) is expressed as

$$\hat{q} = P(\omega,\beta)\hat{u}$$

and the second constraint becomes the constraint in (8). From the definition of phasor, one has (9).

Using Lemma 7.1 in Appendix, it can be verified that the objective function in (6) is given by

$$\begin{aligned}\frac{1}{T}\int_0^T \begin{bmatrix} q \\ u \end{bmatrix}^\intercal \overset{o}{\Pi} \begin{bmatrix} q \\ u \end{bmatrix} dt &= \frac{1}{2}\begin{bmatrix} \hat{q} \\ \hat{u} \end{bmatrix}^* \Pi(j\omega) \begin{bmatrix} \hat{q} \\ \hat{u} \end{bmatrix} \\ &= \frac{1}{2}\begin{bmatrix} P(\omega,\beta)\hat{u} \\ \hat{u} \end{bmatrix}^* \Pi(j\omega) \begin{bmatrix} P(\omega,\beta)\hat{u} \\ \hat{u} \end{bmatrix} \\ &= \hat{u}^* X(\omega,\beta)\hat{u}.\end{aligned}$$

The equivalence between (6) and (8) is thus proved. ■

Constrained quadratic optimization problems are often hard to solve and require solvers to get the exact solution. However, it is easy to show the exact, analytical solution in our case because of a simpler nature of problem.

Theorem 4.1: Consider the system (4) with an explicit $N(\alpha,\beta)$ for $\alpha,\beta \in \mathbb{R}^+$. Let

$$\omega_n, z_n = \alpha \begin{bmatrix} 1 \\ \beta_n \\ -\beta_n \\ -1 \end{bmatrix}$$

be the natural frequency and mode shape. Let

$$\omega_o, \beta_o, u_o(t), q_o(t)$$

be the optimal arguments for the optimization problem (6). For the objective function $\Pi(j\omega)$ given in Table II, the following conclusions hold.

(i) If $\mu = 0$,

$$\omega_o = \omega_n, \beta_o = \beta_n, u_o(t) = 0, q_o(t) = \Re[z_n e^{j\omega_n t}]$$

are the optimal arguments for the optimization problem (6).

(ii) As $\mu \to \infty$, there is an optimal argument $\omega_o(\mu)$, explicitly depending on μ, satisfying $\omega_o(\mu) \to 0$.

Proof: By Lemma 4.1, the optimization problem (6) is equivalent to (8). For the objective function $\Pi(j\omega)$ given in Table II, one has

$$X(\omega,\beta) = \frac{1}{2}I \text{ or } \frac{1}{2}\omega^2 I \tag{10}$$

As a result, the objective function can be put in the following form

$$\hat{u}^* X(\omega,\beta)\hat{u} = \frac{1}{2}\|\hat{u}\|^2 \text{ or } \frac{1}{2}\|\omega\hat{u}\|^2.$$

The constraint in (8) can be rewritten as follows

$$\hat{u} = P^{-1}(\omega,\beta)z, \; z := \alpha \begin{bmatrix} 1 \\ \beta \\ -\beta \\ -1 \end{bmatrix}.$$

As a result, the optimization problem (8) reduces to

$$\min_{\substack{\omega,\beta\in\mathbb{R}^+\\ \hat{u}\in\mathbb{C}^n}} \frac{1}{2}\|\hat{u}\|^2 \text{ or } \frac{1}{2}\|\omega\hat{u}\|^2 \text{ subject to}$$

$$\hat{u} = (K_o + G_o - N(\alpha,\beta) + j\omega\mu J - \omega^2 J)z. \tag{11}$$

The equations in (9) become

$$u(t) = \Re[\hat{u}e^{j\omega t}], \quad q(t) = \Re[ze^{j\omega t}]. \tag{12}$$

Case (i) with $\mu = 0$: From the definition of natural frequency and mode shape, one has

$$(K_o + G_o - N(\alpha,\beta_n) - \omega_n^2 J)z_n = 0.$$

With $\omega = \omega_n, \beta = \beta_n, z = z_n$, one has $\hat{u} = 0$ and

$$\frac{1}{2}\|\hat{u}\|^2 \text{ or } \frac{1}{2}\|\omega\hat{u}\|^2 = 0$$

achieving the optimal value. It concludes that

$$\omega_o = \omega_n, \beta_o = \beta_n, \hat{u}_o = 0$$

are the optimal arguments for the optimization problem (11) and hence (8). Moreover, by (12),

$$\omega_o = \omega_n, \beta_o = \beta_n, u_o(t) = 0, q_o(t) = \Re[z_n e^{j\omega_n t}]$$

are the optimal arguments for the optimization problem (6).

Case (ii) with $\mu \to \infty$: For

$$X(\omega,\beta) = \frac{1}{2}\omega^2 I,$$

$\omega_o = 0$ is always an optimal argument for the optimization problem (11). So, the remaining proof is only for

$$X(\omega,\beta) = \frac{1}{2}I.$$

In particular, the optimization problem (11) becomes

$$\min_{\omega,\beta\in\mathbb{R}^+} \|(K_o + G_o - N(\alpha,\beta) + j\omega\mu J - \omega^2 J)z\| \tag{13}$$

that is equivalent to

$$\min_{\omega,\beta\in\mathbb{R}^+} \|(K_o + G_o - N(\alpha,\beta) - \omega^2 J)z\|/\mu + \|\omega J z\|. \tag{14}$$

As $\mu \to \infty$, it reduces to

$$\min_{\omega,\beta\in\mathbb{R}^+} \|\omega J z\| \tag{15}$$

which gives an optimal argument $\omega_o = 0$. ■

The results in Theorem 4.1 show that, when the damping factor μ is small, the natural oscillation is approximately an

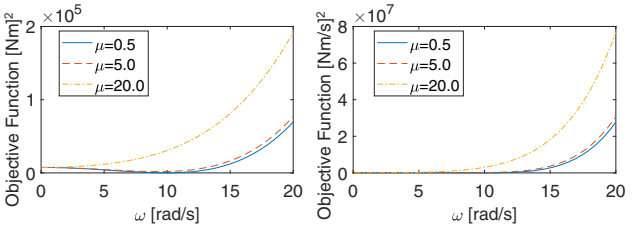

Fig. 2. Input torque (left) and input torque rate (right) versus frequency for a two-link system.

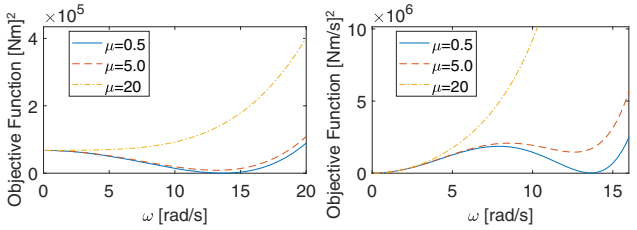

Fig. 3. Input torque (left) and input torque rate (right) versus frequency for a four-link system.

optimal oscillation in term of minimizing the input torque or the input torque rate. In other words, the natural oscillation is persistent without a significant amount of input, noting $u_o(t) = 0$. However, when the damping factor μ becomes larger, the optimal frequency may be significantly reduced, in particular, to zero when μ approaches infinity.

V. Numerical Simulation

Frequency sweep was used to find the local minima in the feasible set of frequencies for the biped. All the parameters in this simulation were kept as nominal parameters in Table I unless otherwise specified. The optimal frequency turns out to be consistent with the natural frequency for the specified objective functions. The results of the simulation are summarized in the Table III for different stiffness parameter k_o with a small $\mu = 0.5$. As expected by Theorem 4.1, Figures 2 and 3 show that, when μ is small, the optimal frequency is approximated by the natural frequency for the optimization problem; as μ becomes larger the optimal frequency moves closer to zero. It also noted that 0 is always another (trivial) optimal frequency for the minimizing the input torque rate.

TABLE III
Natural oscillation frequency vs Optimal frequency)

	two-link		four-link	
k_o (Nm/rad)	50	100	250	500
Natural (rad/s) ω_n	9.94	13.37	13.63	18.71
Opt. (i/p torque) (rad/s) ω_o	9.90	13.40	13.60	18.70
Opt. (i/p torque rate) (rad/s) ω_o	9.90	13.40	13.60	18.70

Next, the amplitude (α) was also varied with nominal parameters. As it turns out, amplitude causes the least of variations. Hence, it was kept constant and instead the amplitude-ratio β was varied for the four-link system. The results are shown in Figure 4 with their minima highlighted. These graphs show that the minima of the objective function

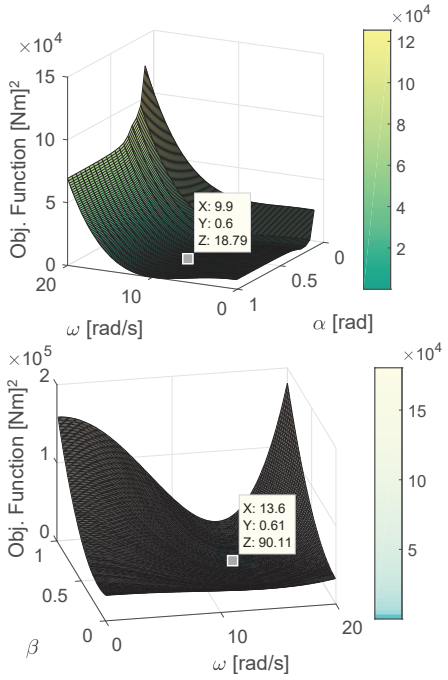

Fig. 4. Input torque versus frequency and amplitude for two-link (top), and input torque versus frequency and amplitude-ratio for four-link (bottom) models.

(for input torque) given by

$$\min_{\substack{\omega,\beta\in\mathbb{R}^+\\ \hat{u}\in\mathbb{C}^n}} \frac{1}{2}\|\hat{u}\|^2$$

turns out to be $18.79(Nm)^2$ and $90.11(Nm)^2$ for the two-link and the four-link cases, respectively.

The optimal frequency is again close to the natural frequency of the four-link model, and the amplitude-ratio $\beta_o = 0.61$, which is precisely the β_n which ensures consistency of amplitude obtained and the one used in eigenvector/eigenvalue computation shown in preceding work.

Figure 5 shows a time-lapse of the biped gait compared with a famous series of photographs capturing the dynamics of an actual human jogging. Amplitude angles (α) of thigh and shank can be measured from these snapshots, from where we can calculate the parameter β for this individual: $\alpha_1 = 54.16^o$, $\alpha_2 = 31.43^o$, and $\beta = 0.58$.

Tables IV and V gives us an interesting insight into the parameters governing the dynamics of the biped. Table IV shows the effect on β with change in the parameters, such as mass and length, but with the moment of inertia kept constant. This means if the length is increased to twice its nominal value, then the mass would have to be decreased four times its nominal value to ensure a constant moment of inertia and vice versa. This is consistent with the expression of the moment of inertia of a pendulum which is ml^2. For the results in Table V the leg length was kept constant whereas the masses were varied just as they were varied previously. The results show significant variation in β which ranges between 0.53-0.72. The results from these two tables also suffices to show that β is independent of mass and length

of each link, but rather depends on the ratio of moment of inertia of upper and lower links. Also, the value of β obtained from the actual human measurements above fall in between this range and is close to the optimal and the natural value of β_n. This further validates that our model, and the gait obtained from the present model and its parameters, are close to human locomotion profile.

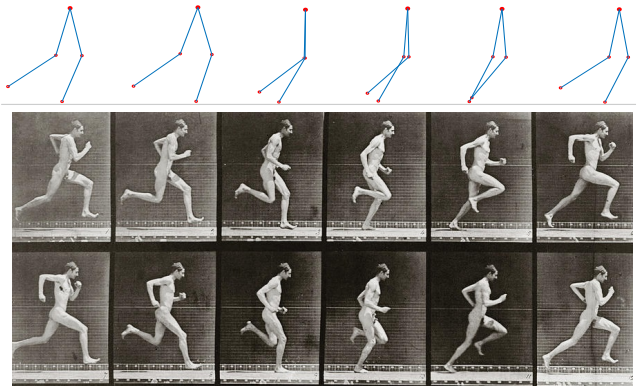

Fig. 5. Simulation of the biped model in natural oscillation and motion of a man jogging as captured by Eadweard Muybridge in 19th century.

TABLE IV

EFFECT OF β WITH VARIATION IN PARAMETERS

m_2 and m_3 (kg)	b_2 and b_3 (m)	α_1 (rad.)	α_2 (rad.)	β
10	$\sqrt{2} \times 0.25$	0.789	0.502	0.63
15	$\sqrt{1.333} \times 0.25$	0.79	0.500	0.63
20	$\sqrt{1} \times 0.25$	0.789	0.499	0.63
25	$\sqrt{0.8} \times 0.25$	0.79	0.498	0.63
30	$\sqrt{0.667} \times 0.25$	0.79	0.496	0.63

TABLE V

VARIATION OF β WITH CHANGE IN PARAMETERS

m_1 and m_4 (kg)	m_2/m_1	α_1 (rad.)	α_2 (rad.)	β
2	10	0.753	0.538	0.72
4	5	0.791	0.499	0.63
6	3.33	0.815	0.483	0.59
8	2.5	0.876	0.466	0.53
10	2	0.815	0.455	0.56

VI. CONCLUSION

Simplified continuous models for the two-link and four-link planar biped robots were presented. The models were approximated using the describing function analysis. An objective function was formulated for the biped upon minimization of which had given us the optimal gait. It turns out the natural gait is also the optimal gait for minimizing the control input torque or torque rate. The optimal frequency reduces to compensate for damping. This was further verified using extensive simulations.

VII. APPENDIX

Lemma 7.1: [19] Let a positive $T \in \mathbb{R}$, a vector valued function $\mu \in \mathbb{P}_T$ be given, and a set of transfer functions $\Pi(s)$ of the form $\Pi(s) = F(-s)^\intercal \Phi F(s)$ where Φ is a constant Hermitian matrix and $F(s)$ is a linear combination of stable (proper) transfer functions and differentiators. Let ξ be the steady state response of $F(s)$ with sinusoidal input μ. Then the following hold:

$$\hat{\xi} = F(j\omega)\hat{\mu}, \ \frac{2}{T}\int_0^T \mu^\intercal \overset{o}{\Pi} \mu dt = \hat{\mu}^* \Pi(j\omega)\hat{\mu},$$

where $\hat{\xi}$ and $\hat{\mu}$ represent the phasors of their respective sinusoidal signals.

REFERENCES

[1] Y. Hurmuzlu, F. Genot, and B. Brogliato, "Modeling, stability and control of biped robots - a general framework," *Automatica*, vol. 40, no. 10, pp. 1647 – 1664, 2004.

[2] J. W. Grizzle, C. Chevallereau, R. W. Sinnet, and A. D. Ames, "Models, feedback control, and open problems of 3d bipedal robotic walking," *Automatica*, vol. 50, no. 8, pp. 1955 – 1988, 2014.

[3] T. McGeer, "Passive dynamic walking," *The International Journal of Robotics Research*, vol. 9, no. 2, pp. 62–82, 1990.

[4] A. Goswami, B. Espiau, and A. Keramane, "Limit cycles in a passive compass gait biped and passivity-mimicking control laws," *Autonomous Robots*, vol. 4, no. 3, pp. 273–286, 1997.

[5] Y. Hu, G. Yan, and Z. Lin, "Stable running of a planar underactuated biped robot," *Robotica*, vol. 29, pp. 657–665, 9 2011.

[6] C. Tang, G. Yan, and Z. Lin, "Walking control for compass-like biped robot with underactuated ankle," *Transactions of the Institute of Measurement and Control*, pp. 3852–3857, July 2012.

[7] Z. J. Jackowski, "Design, construction, and experiments with a compass gait walking robot," Ph.D. dissertation, Massachusetts Institute of Technology, 2011.

[8] P. B. Wieber, "Trajectory free linear model predictive control for stable walking in the presence of strong perturbations," in *2006 6th IEEE-RAS International Conference on Humanoid Robots*, Dec 2006, pp. 137–142.

[9] J. Carpentier, S. Tonneau, M. Naveau, O. Stasse, and N. Mansard, "A versatile and efficient pattern generator for generalized legged locomotion," in *2016 IEEE International Conference on Robotics and Automation (ICRA)*, May 2016, pp. 3555–3561.

[10] B. Ponton, A. Herzog, S. Schaal, and L. Righetti, "A convex model of humanoid momentum dynamics for multi-contact motion generation," in *2016 IEEE-RAS 16th International Conference on Humanoid Robots (Humanoids)*, Nov 2016, pp. 842–849.

[11] E. R. Westervelt, J. W. Grizzle, and D. E. Koditschek, "Hybrid zero dynamics of planar biped walkers," *IEEE Transactions on Automatic Control*, vol. 48, no. 1, pp. 42–56, Jan 2003.

[12] D. Koop and C. Q. Wu, "Passive dynamic biped walking part i: Development and validation of an advanced model," *Journal of Computational and Nonlinear Dynamics*, vol. 8, no. 4, p. 041007, 2013.

[13] U. I. Khan and Z. Chen, "Natural oscillation gait in humanoid biped locomotion," *IEEE Transactions on Control Systems Technology [submitted]*, 2017.

[14] L. Zhu, Z. Chen, and T. Iwasaki, "Oscillation, orientation, and locomotion of underactuated multilink mechanical systems," *IEEE Transactions on Control Systems Technology*, vol. 21, no. 5, pp. 1537–1548, Sept 2013.

[15] Z. Chen, T. Iwasaki, and L. Zhu, "Feedback control for natural oscillations of locomotion systems under continuous interactions with environment," *IEEE Transactions on Control Systems Technology*, vol. 23, no. 4, pp. 1294–1306, July 2015.

[16] G. Bessonnet, S. Chesse, and P. Sardain, "Optimal gait synthesis of a seven-link planar biped," *The International journal of robotics research*, vol. 23, no. 10-11, pp. 1059–1073, 2004.

[17] J. P. Ostrowski, J. P. Desai, and V. Kumar, "Optimal gait selection for nonholonomic locomotion systems," *The International journal of robotics research*, vol. 19, no. 3, pp. 225–237, 2000.

[18] T. Saidouni and G. Bessonnet, "Generating globally optimised sagittal gait cycles of a biped robot," *Robotica*, vol. 21, no. 2, pp. 199–210, 2003.

[19] J. Blair and T. Iwasaki, "Optimal gaits for mechanical rectifier systems," *IEEE Transactions on Automatic Control*, vol. 56, no. 1, pp. 59–71, 2011.